PHYSICAL REVIEW B

CONDENSED MATTER AND MATERIALS PHYSICS

THIRD SERIES, VOLUME 61, NUMBER 10 1 MARCH 2000-II

RAPID COMMUNICATIONS

Rapid Communications are intended for the accelerated publication of important new results and are therefore given priority treatment both in the editorial office and in production. A Rapid Communication in **Physical Review B** *may be no longer than four printed pages and must be accompanied by an abstract. Page proofs are sent to authors.*

Ferroelectric $PbTiO_3/BaTiO_3$ superlattices: Growth anomalies and confined modes

F. Le Marrec, R. Farhi, M. El Marssi, J. L. Dellis, and M. G. Karkut
LPMC, Université de Picardie Jules Verne, 33 rue Saint Leu, F-80039 Amiens, France

D. Ariosa
Department of Physics, Swiss Federal Institute of Technology, CH-1015 Lausanne, Switzerland
(Received 12 August 1999)

We have used laser ablation to grow series of $PbTiO_3/BaTiO_3$ (PTO/BTO) multilayers with a modulation wavelength Λ that varies between $50\ \text{Å} < \Lambda < 360\ \text{Å}$. Modeling the x-ray-diffraction patterns of the multilayers indicates that the PTO layers are *a*-axis oriented. The Raman measurements reinforce this interpretation. The soft-mode Raman line shifts abruptly in frequency above $\Lambda = 240\ \text{Å}$ due to possible strain relaxation of the multilayer, and the Λ dependent position of an asymmetric line in the vicinity of 200 cm^{-1} is modeled as a confined mode, a signature of a modulated structure.

Lead titanate [$PbTiO_3$(PTO)] is among the best known and most studied of the ferroelectric oxides. Its Curie temperature $T_C = 493\,^\circ\text{C}$ at which it undergoes a cubic to tetragonal structural transition, was reported nearly 50 years ago.[1] And yet it still continues to receive a great deal of attention both theoretically and experimentally. It has been the subject of a first-principles calculation[2] using a Berry's phase approach to calculate the piezoelectric constants of PTO, and Pertsev *et al.*[3] has used a thermodynamic approach, to construct a phase diagram of epitaxial PTO thin films in which the polarization can be in or out of the plane of the film depending on the lattice mismatch with the substrate. The epitaxial growth of PTO and domain formation on different substrates has been investigated by x-ray diffractometry.[4,5] Lattice mismatch was also the subject of experimental Raman studies[6,7,8] on oriented PTO films on different substrates. In Ref. 6 it was shown that the internal strains reduced the Curie temperature of the ferroelectric transition, as theoretically expected.[9] This was done by monitoring the soft mode with temperature. One reason for this research activity on PTO is the important role size will play in the potential realization of oxide-based devices, and hence the necessity to understand the physics of small scale ferroelectric thin-film heterostructures and their mechanical relation with the substrates.

We have used PTO along with another ferroelectric perovskite $BaTiO_3$ (BTO), $T_C = 118\,^\circ\text{C}$ to fabricate a series of superlattices with modulation wavelengths varying between 48 Å and 356 Å. Superlattices consisting of semiconductors, of superconductors, of magnetic materials have long been the subject of fruitful inquiry, but it is only recently that ferroelectric superlattices have begun to be exploited. The focus is not only to construct artificial structures with properties superior to those of the constituents, such as the high dielectric constant BTO/STO multilayers[10] and related materials grown by Tabata and Kawai, but also to investigate the effect of size on the ferroelectric transition. Specht *et al.*[11] grew $KNbO_3/KTaO_3$ multilayers and observed a decrease in T_C with decreasing layer thickness before interlayer coupling became significant at short modulation wavelengths. Our study here uses the Raman techniques in Ref. 6 along with x-ray diffractometry to investigate the properties of ultrathin ferroelectrics. Raman scattering has been a useful tool not only in investigating the strains in thin films[6] but also in investigating the vibration spectra of semiconductor superlattices.[12] In superlattices, optical modes can be confined within individual layers giving rise to the observation of discrete frequencies. It is not unreasonable to expect that such confined modes could exist in ferroelectric superlattices as well. In this letter, we present x-ray-diffraction, x-ray modeling, and Raman-scattering results of PTO/BTO superlattices grown on (100) MgO buffered with 50 Å of STO.

The films were deposited using pulsed laser ablation in a UHV chamber equipped with a 15 kV reflection high-energy

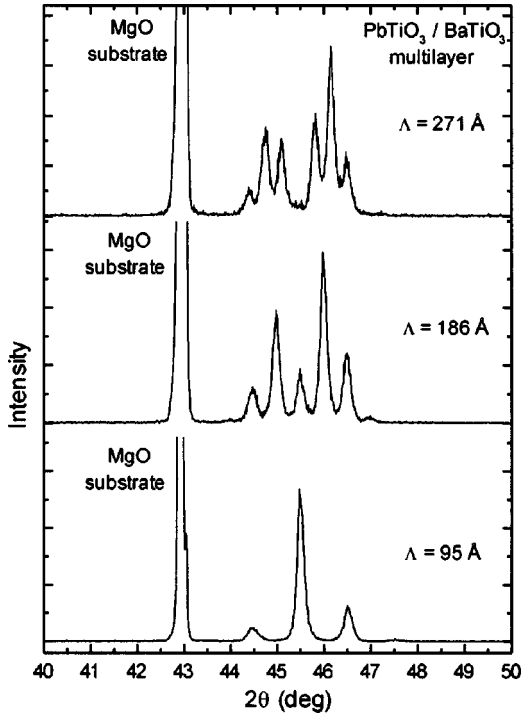

FIG. 1. The evolution of the θ-2θ x-ray-diffraction pattern for three PTO/BTO superlattices as a function of the modulation period Λ.

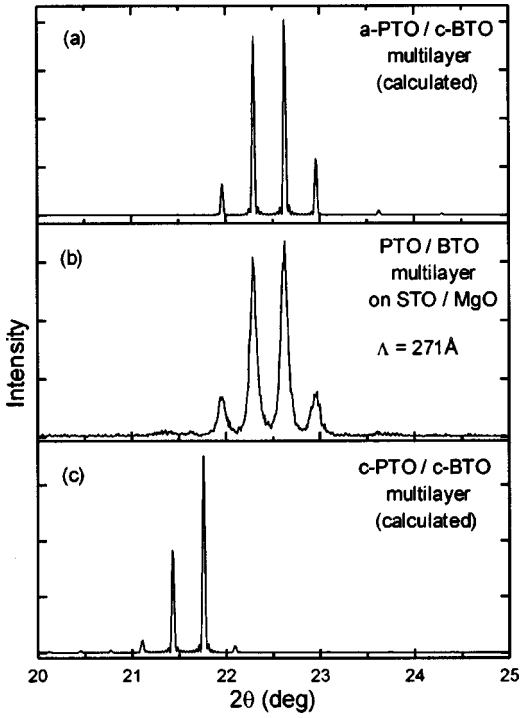

FIG. 2. The θ-2θ diffractogram of the 271 Å multilayer (b), along with calculations for a model 271 Å wavelength *a*-domain PTO/*c*-domain BTO multilayer (a), and a *c*-domain PTO/*c*-domain BTO multilayer (c).

electron diffraction (RHEED) system. The 50 Å STO buffer layer was deposited at a substrate temperature T_s of 800 °C with a partial pressure of oxygen P_{O2} of 10^{-3} mbar. The PTO and BTO layers were deposited at $T_s = 640\,°C$ and $P_{O2} = 0.1$ mbar. The total multilayer thicknesses were 3800 Å. RHEED streaks, indicative of an atomically smooth surface, were observed for all films presented in this study. More details on the deposition and experimental procedures may be found in Ref. 13.

All samples were studied by θ-2θ x-ray diffraction. The bulk lattice parameters for PTO are $c = 4.15$ Å, $a = 3.899$ Å, for BTO: $c = 4.04$ Å, $a = 3.99$ Å, for STO: $a = 3.905$ Å, and for MgO: $a = 4.213$ Å. It is known[4,5] that PTO deposited directly on MgO results in *c*- and *a*-domain regions. Using STO single-crystal substrates we have grown very high quality PTO films with rocking curves of 0.1° full width at half maximum (FWHM). However, STO gives a very strong Raman signal background which overwhelms any response from the thin film. Thus we used cubic MgO as a substrate, which is not Raman active, after buffering it with 50 Å of STO to promote single *c*-domain growth of the ferroelectric oxides. Individual 2000 Å thin films of PTO and BTO on STO buffered MgO are grown using the same deposition conditions as the multilayers. X-ray diffraction indicates predominant *c*-axis orientation with less than 4% of *a*-domain structure. For the multilayers, we observe the so-called satellite peaks, indicative of modulated structures, as well as their evolution as a function of Λ. Figure 1 displays three multilayer samples with wavelengths of 95, 186, and 271 Å. It is clear from this figure that it is not possible to assign a ''main'' peak to the PTO layers and a ''main'' peak to the BTO layers, and then assign the rest to satellite status. A useful way to think about the diffractograms is that the entire superlattice structure diffracts the x-rays and that the intensities of the diffracted peaks are modulated by the structure factor of the bilayer ($PTO_{\Lambda/2}/BTO_{\Lambda/2}$), which is the unit cell of a superlattice of period Λ. The structure factor is very sensitive to the lattice parameters, to the size of the multilayer period and to the diffraction angle. The peak positions are given by Bragg condition $\sin\theta_n = n\lambda_x/2\Lambda$, where n is an integer and $\lambda_x = 1.5406$ Å is the x-ray wavelength, and so Λ is given by the separation of the adjacent peaks: $\Lambda = \lambda_x/2(\sin\theta_{n+1} - \sin\theta_n)$. We have performed model calculations based on standard x-ray-diffraction theory[14] in which we calculate the diffraction amplitude in a specular geometry using the interplanar spacings of the PTO and BTO as well as their individual thicknesses in each bilayer as the adjustable parameters. The results are surprising. Our model clearly favors a superlattice structure in which the PTO layers are oriented with the *a* axis parallel to the growth direction and the BTO layers *c*-axis oriented. This contrasts sharply with single thin PTO (170 Å thick) films and 170 Å/170 Å thick PTO/BTO bilayers we have subsequently grown, for which we observe only *c*-axis growth. The high quality of the fits is evident in Fig. 2 which shows the diffractogram of the 271 Å superlattice along with two model calculations. The calculated x-ray intensities for a 271 Å multilayer consisting of *a*-axis PTO layers and *c*-axis BTO layers convincingly fits the experimental data whereas the predictions of the *c*-axis/*c*-axis model (as well as *a*-axis/*a*-axis and *c*-axis/*a*-axis models not displayed here) are inadequate. All the superlattices presented in this study have been successfully fit with this *a*-axis PTO/*c*-axis BTO multilayer model with $a(\mathrm{PTO}) = 3.93$ Å and $c(\mathrm{BTO}) = 4.04$ Å. If we take into account only the elastic energy of

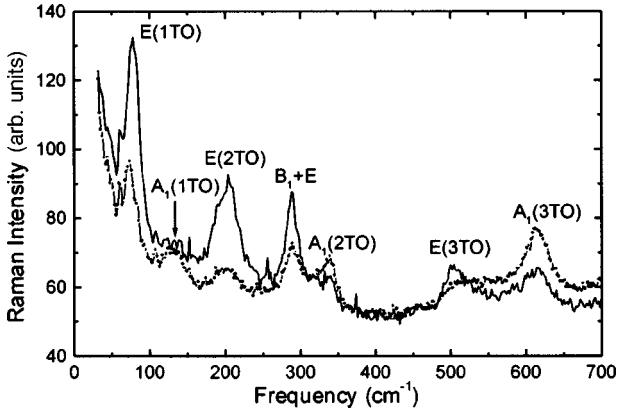

FIG. 3. Crossed (solid line) and parallel (circles) polarization room-temperature Raman spectra for the $\Lambda = 356$ Å PTO/BTO multilayer. The modes are labeled according to the assignments in Table I.

the heterostructure, then based on lattice matching conditions, we would expect the multilayer to be *c*-axis orientated, which is indeed the case for the above-mentioned thin films and PTO/BTO bilayers. Our *a*-axis growth anomaly would seem to be the result of the changing energy balance between the elastic strains and the polarization as we go from bilayer to multilayer structures. The calculations of Ref. 3 show that this balance can change the polar orientation of ferroelectric PTO thin films from parallel to perpendicular depending on the mismatch between film and substrate. However, this work considers only single films. Theoretical work is now in progress[15] to treat the case of ferroelectric multilayers. Additional thin film experiments are also underway in an attempt to understand the origin of this PTO/BTO multilayer anomaly.

We now turn to the Raman measurements, which give the frequencies of the various lattice vibration modes via the inelastic scattering of light. The Raman spectra were recorded in backscattering geometry using a microprobe device which focuses the laser beam to a spot of 2 micrometers in diameter. The spectral resolution was set to 3 cm^{-1}. We observe only PTO modes in the multilayer Raman spectra and this reinforces our x-ray derived interpretation of *a*-domain PTO layers. The way in which Raman selection rules are observed reflects the epitaxial character of the sample. For example, in mixed *c*- and *a*-domain PTO films, all Raman lines are present for whatever the light polarization,[6] whereas we observe selection rules for epitaxial lead zirconate titanate (PZT) thin films, but no selection rules for PZT ceramics.[13] We present in Fig. 3 the room-temperature Raman spectra of a 356 Å period PTO/BTO superlattice in crossed and parallel polarizations of the incident and scattered light. For a *c* domain having the C_{4v} point group, parallel $z(xx)\bar{z}$ or $z(yy)\bar{z}$ spectra will consist only of weak $A_1(LO)$ and B_1 modes and crossed $z(xy)\bar{z}$ spectra should not show any lines. If the domains are *a* oriented, and considering for the time being the same C_{4v} point group, crossed $x(yz)\bar{x}$ spectra will show $E(TO)$ and $E(LO)$ modes, parallel $x(yy)\bar{x}$ spectra will give rise to $A_1(TO)$ and B_1 lines, and parallel $x(zz)\bar{x}$ spectra will present $A_1(TO)$ lines only. These considerations, along with our x-ray analysis that the PTO and BTO layers are *a* and *c* oriented, respectively, and thus explain the presence only of PTO modes. Table I is a listing of (a) the mode assignments according to Ref. 16, (b) the frequencies observed for a bulk single crystal of PTO (Ref. 17), (c) our measured frequencies for the 356 Å multilayer, and (d) the Grüneisen parameters $(d\omega/dP)$ from a high-pressure study on PTO single crystal.[18] The comparison in Table I of the measured superlattice frequencies with those of bulk lead titanate is unambiguous and reinforces the interpretation of *a*-oriented PTO layers in the superlattice. Although there is a one to one correspondence in Table I between our data and the single-crystal data, there are also significant frequency shifts present for some lines between the two sets of data. Such differences in Raman spectra have been attributed[6–8] to the effect of internal stresses. The lines most sensitive to pressure (Table I) are $E(1TO)$, $A_1(1TO)$, $A_1(2TO)$ and $A_1(3TO)$. These lines are indeed shifted for the multilayer sample.

TABLE I. Mode labeling, frequencies (in cm^{-1}), and Grüneisen constants.

Mode labeling[a]	Single crystal PTO[b]	Multilayer[c]	Grüneisen parameter[d]
$E(1TO)$	87.5	78	−5.8
$A_1(1TO)$	148.5	130	−6.97
$E(2TO)$	218.5	202	−2.3
B_1+E	289	289	−1.38
$A_1(2TO)$	359.5	338	−15.17
$E(3TO)$	505	503	7.14
$A_1(3TO)$	647	615	−16.9

[a]For PTO single crystal. Reference 16.
[b]For PTO single crystal. Reference 17.
[c]Present work. $\Lambda = 356$ Å.
[d]$d\omega/dP$ for PTO single crystal. Reference 18.

In Fig. 4 we present Raman spectra between 20 and 400 cm^{-1} for seven different PTO/BTO superlattices. The spectra have been recorded in crossed light polarization. For the stress-induced frequency-shifted $E(1TO)$ and $A_1(2TO)$ modes, an abrupt jump to a higher frequency, from 72 to 78 cm^{-1} for the $E(1TO)$ and from 324 to 340 cm^{-1} for the $A_1(2TO)$, is observed for the $\Lambda = 310$ and 356 Å superlattices. This could be associated with a partial relaxation of the stresses at a critical wavelength Λ_c, above which it is energetically more favorable for misfit dislocations to relieve the strain.[19] An elastic energy calculation, based on Ref. 19, yields $\Lambda_c = 150$ Å for a PTO/BTO superlattice, in agreement with the Raman results.

The most striking feature of Fig. 4 is the large shift of the $E(2TO)$ line and its continuous variation with Λ. Such a large frequency shift cannot be due to stress effects alone since the low Grüneisen parameter value for this mode would seem to preclude such an explanation. Moreover, this line is broader and more asymmetric than the other lines. Raman scattering from superlattices has been extensively studied in GaAs/AlAs multiple quantum wells.[12] For a wave vector normal to the layers, and no overlap of the phonon-dispersion curves of the constituent materials, the modes cannot propagate throughout the superlattice and are confined to individual layers.[20] Raman spectra will show lines at

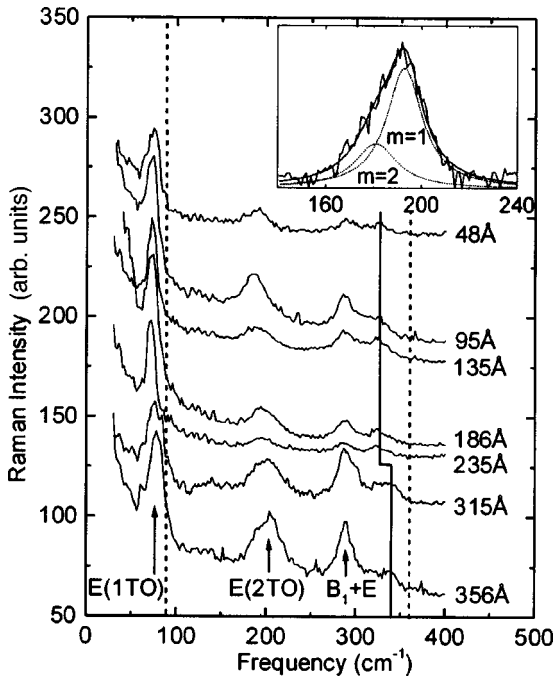

FIG. 4. Crossed polarization Raman spectra for seven different PTO/BTO multilayer samples. The dashed lines indicate the measured frequencies for the $E(1TO)$ and the $A_1(2TO)$ modes of single-crystal PTO. The solid line follows the abrupt jump in frequency for the $A_1(2TO)$ mode. The Raman line in the vicinity of 200 cm^{-1} is strongly Λ dependent. Inset: Deconvolution of the Λ dependent line for the $\Lambda = 48$ Å multilayer.

frequencies $\omega(\mathbf{q})$ with $\mathbf{q}=(m\pi/d)\mathbf{n}$, where d is the thickness of the layer, m is an integer, $\mathbf{n}$ is the normal to the layers, and $\omega(\mathbf{q})$ is the dispersion relation for the bulk material. The large width of the $E(2TO)$ line, together with its Λ dependent shift, strongly suggests that it is made up of confined modes which overlap due to their rather large damping. The point group of the *a*-oriented PTO/*c*-oriented BTO superlattice is not C_{4v}, but C_S. Thus crossed polarized spectra result in the observation of $A''(TO)$ modes and by symmetry all orders of m are allowed. The interval between successive quantized values of $|\mathbf{q}|$ increases on decreasing Λ, which means that the first-order wave vector is rather far from the Brillouin-zone center for small Λ. Because the intensity of the confined modes is higher for the smallest m values,[20] we expect the distribution of this ''confined modes'' line to shift towards the bulk frequency of the PTO $E(2TO)$ mode with increasing Λ. In addition, the variation of this shift with Λ should map the bulk phonon-dispersion curve for PTO. For ω decreasing with q, we expect the shift of the modes to increase with Λ, which is what we observe in Fig. 4. A negative dispersion has in fact been calculated for this mode using a rigid-ion approximation.[21] By the same arguments this broad line should also be asymmetric. The insert in Fig. 4 shows the ''confined modes'' line for a 48 Å period superlattice recorded with higher resolution and an improved signal to noise ratio. Because of the large linewidth of individual modes, successive orders could not be distinctly separated, but the line can be fit by two lorentzians centered at 193.6 and 181.8 cm^{-1} that we attribute to the $m=1$ and $m=2$ orders, respectively. Considering a linear dispersion relation[21] the extrapolation to $q=0$ would give a frequency of 205.4 cm^{-1}, in good agreement with that found for this mode in pure PTO thin films.[6,7]

In conclusion, we have grown a series of ferroelectric superlattices and we propose, based on the excellent correspondence between x-ray diffractograms and a multilayer diffraction model, that the structure is *a*-domain PTO and *c*-domain BTO. This interpretation is strongly reinforced by the Raman study in which we observe only PTO modes and no BTO modes for the multilayers spectra. In addition, we observe a Λ dependent mode which can be modeled as confined vibrational modes in the PTO layers. These multilayer effects could shed additional light on the physics of the ferroelectric size effect and may also have technological implications for device construction.

We thank V. Lorman and L. Lahoche for enlightening discussions and Paula Vilarinho for supplying a PTO target. We gratefully acknowledge the Region of Picardy and the European Social Fund for financial support.

[1] G. Shirane, S. Hoshino, and K. Suzuki, Phys. Rev. **80**, 1105 (1950).
[2] G. Saghi-Szabo, R. E. Cohen, and H. Krakauer, Phys. Rev. Lett. **80**, 4321 (1998).
[3] N. A. Pertsev, A. G. Zembilgotov, and A. K. Tagantsev, Phys. Rev. Lett. **80**, 1988 (1998).
[4] C. M. Foster *et al.*, J. Appl. Phys. **78**, 2607 (1995).
[5] B. S. Kwak *et al.*, Phys. Rev. B **49**, 14 865 (1994).
[6] Y. Yuzyuk *et al.*, J. Appl. Phys. **84**, 452 (1998).
[7] I. Taguchi *et al.*, J. Appl. Phys. **73**, 394 (1993).
[8] L. Sun *et al.*, Phys. Rev. B **55**, 12 218 (1997).
[9] G. A. Rossetti, L. E. Cross, and K. Kushida, Appl. Phys. Lett. **59**, 2524 (1991).
[10] H. Tabata and T. Kawai, Appl. Phys. Lett. **70**, 321 (1997).
[11] E. D. Specht *et al.*, Phys. Rev. Lett. **80**, 4317 (1998).
[12] See, for example, T. Ruf, *Phonon Raman Scattering in Semiconductors, Quantum Wells, and Superlattices* (Springer, Berlin, 1998).
[13] M. Karkut *et al.*, Ferroelectrics **225**, 1067 (1999).
[14] See, for example, I. K. Schuller, Phys. Rev. Lett. **44**, 1597 (1980).
[15] M. Glinchuk and V. Stepanovitch (private communication).
[16] G. Burns and B. Scott, Phys. Rev. B **7**, 3088 (1973).
[17] C. M. Foster *et al.*, Phys. Rev. B **48**, 10 160 (1993).
[18] J. A. Sanjurjo, E. Lopez-Cruz, and G. Burns, Phys. Rev. B **28**, 7260 (1983).
[19] For a discussion see, for example, D. Ariosa *et al.*, Phys. Rev. B **37**, 2415 (1988).
[20] A. K. Sood *et al.*, Phys. Rev. Lett. **54**, 2111 (1985).
[21] J. Freire and R. Katiyar, Phys. Rev. B **37**, 2074 (1988).